Afrique SCIENCE *24(6) (2024) 86 - 95*
ISSN 1813-548X, http://www.afriquescience.net

Optimization of $NdRuO_3$ perovskite based photoanodes to improve the efficiency of natural dye solar cells

Assohoun Fulgence KRAIDY[1*], Simon Abe YAPI[2], Koffi Joseph DATTE[2], Mimoun El MARSSI[1] et Yaovi GAGOU[1]

[1] University of Picardie Jules Verne, 33 rue Saint Leu, 80039 Amiens cedex 01, LPMC, France
[2] Université Felix Houphouët Boigny, UFR SSMT, Lab-Tech, Abidjan, Côte d'Ivoire

(Reçu le 02 Mars 2024 ; Accepté le 14 Avril 2024)

* Correspondance, courriel : *fulgence.kraidy@gmail.com*

Abstract

The West African region is renowned for its plethora of plant species harboring natural pigments that exhibit remarkable resistance to temperature fluctuations. Among these, *Baphia nitida*(commonly known as *camwood*) stands out, boasting anthocyanin and coumarin pigments that defy degradation. Abundant in Côte d'Ivoire, the utilization of this plant promises not only to enhance the efficacy of our newly developed perovskites but also to streamline production costs owing to its widespread availability. This article delves into the optimization of material performance and solar architecture through numerical simulation. For the first time, we introduce oxide perovskite neodymium ruthenate ($NdRuO_3$) as an electron transport layer (ETL) in conjunction with a natural dye, 3,3-methylene-bis (4-hydroxycoumarin). Moreover, we are exploring the replacement of the I^-/I^{3-} redox electrolyte with a Spiro-OmeTAD hole transport layer (HTL) to address stability concerns in dye-sensitized solar cells (DSSCs). The simulated device (FTO/$NdRuO_3$/bis-coumarin/Spiro-OmeTAD/Au) is configured in a planar p-i-n architecture, allowing for a meticulous examination of parameter variations such as operating temperature, $NdRuO_3$ photoanode thickness, and defect density on cell performance. Remarkably, we achieved an efficiency (η) of 19.61 % with a $NdRuO_3$ photoanode thickness of 0.5µm^2, an open circuit voltage of 158.26 mV, a short-circuit current (J_{sc}) of 14.71 mA/cm^2, and a fill factor (FF) of 84.19 %. Exploring the thickness variation of the inorganic perovskite structure ($NdRuO_3$) while maintaining the initial parameters of other materials yielded a groundbreaking efficiency of 20.73 % for a thickness of 2 µm. However, this was accompanied by a decrease in the fill factor (FF) to 83.53 %, indicating a lower quality of the simulated DSSC cell.

Keywords : *DSSC, SCAPS 1D simulation, photoanodes, inorganic perovskites.*

Résumé

Optimisation des photoanodes à base de pérovskite $NdRuO_3$ pour améliorer l'efficacité des cellules solaires à colorant naturel

La région de l'Afrique de l'Ouest est réputée pour sa pléthore d'espèces végétales abritant des pigments naturels qui présentent une résistance remarquable aux fluctuations de température. Parmi ces espèces, *Baphia nitida* se distingue par ses pigments anthocyanes et coumarines qui se dégradent dans une longue durée. Abondante en Côte d'Ivoire, l'utilisation de cette plante promet non seulement d'améliorer l'efficacité

de nos pérovskites nouvellement développées, mais aussi de rationaliser les coûts de production grâce à sa grande disponibilité. Cet article se penche sur l'optimisation des performances des matériaux et de l'architecture des cellules solaire par le biais de la simulation numérique. Pour la première fois, nous introduisons la pérovskite d'oxyde ruthénate de néodyme ($NdRuO_3$) comme couche de transport d'électrons (ETL) en association avec un colorant naturel, le 3,3-méthylène-bis (4-hydroxycoumarine). En outre, nous étudions le remplacement de l'électrolyte redox I^-/I^{3-} par une couche de transport de trous Spiro-OmeTAD (HTL) p. Le dispositif simulé (FTO/$NdRuO_3$/bis-coumarine/Spiro-OmeTAD/Au) est configuré dans une architecture p-i-n planaire, ce qui permet un examen méticuleux des variations de paramètres tels que la température de fonctionnement, l'épaisseur de la photoanode $NdRuO_3$ et la densité de défauts sur la performance de la cellule. Nous avons atteint un rendement (η) de 19,61 % avec une épaisseur de photoanode $NdRuO_3$ de 0,5 μm^2, une tension en circuit ouvert de 158,26 mV, un courant de court-circuit (Jsc) de 14,71 mA/cm^2 et un facteur de remplissage (FF) de 84,19 %. L'exploration de la variation de l'épaisseur de la structure pérovskite inorganique ($NdRuO_3$) tout en conservant les paramètres initiaux des autres matériaux a permis d'obtenir un rendement révolutionnaire de 20,73 % pour une épaisseur de 2 µm. Toutefois, ce résultat s'accompagne d'une diminution du facteur de remplissage (FF) à 83,53 %, ce qui indique une basse qualité de la cellule DSSC simulée.

Mots-clés : *DSSC, SCAPS 1D simulation, photoanodes, pérovskites inorganiques.*

1. Introduction

The utilization of an electron transport layer (ETL) with an inorganic perovskite structure in dye-sensitized solar cells (DSSCs) as a substitute for TiO_2, ZnO, or SnO_2 [1 - 4], commonly coupled with a hole transport layer (HTL), represents a promising advancement. This novel approach reduces the dye adhesion time on the electron transport layer while simultaneously enhancing cell efficiency. Phenyl-C61-butyric acid methyl ester (PC61BM) is employed as the electron transport layer along with CuSCN as the hole transport layer, achieving a yield of 5.38 % using the metal dye N719 [5]. Copper iodide (CuI) is utilized as a hole transport layer and compared the performance of various electron transport materials, with TiO_2 exhibiting the highest efficiency at 5.6 % [2]. They proposed that optimizing the combination of CuI and TiO_2 with a perovskite layer could potentially elevate cell efficiency to nearly 30 %. Presently, researchers are exploring alternative metal oxides such as spinel and compounds with an inorganic perovskite structure as potential replacements and/or modifications to the TiO_2 photoanode in DSSC devices [6]. Furthermore, conventional DSSCs typically employ a volatile solvent-based electrolyte such as acetonitrile and a redox couple (I^-/I_3^-). However, the predominant challenge of solution-based solar cells lies in their lack of long-term stability due to issues like liquid leakage, presence of volatile liquids such as acetonitrile, electrode degradation, and dye photodecomposition. In response, researchers are investigating the integration of hole transport materials (HTL). In this context, DSSCs are developed using four different HTL materials, employing Scaps-1D simulation [7]. Among the HTLs tested, CuI demonstrated superior performance compared to others, achieving an efficiency of 17.72 % with the N719 dye [7]. Our objective in this study is to streamline DSSC manufacturing, reduce production costs, enhance efficiency, and ultimately envision the industrial-scale production of environmentally-friendly natural dye solar cells in the near term. To optimize time and minimize waste, we will conduct numerical simulations of this device. Herein, we present the results of an initial simulation of the FTO/TiO_2/$NdRuO_3$/3,3-Methylene-bis(4-hydroxycoumarin)/Spiro-OMeTAD/Au stacking. It is worth noting that TiO_2 serves as a blocking layer, facilitating passivation between the FTO substrate and the $NdRuO_3$ perovskite-structured layer [8]. The 3,3-Methylene-bis(4-hydroxycoumarin), commonly known as dicoumarol [9] can be derived from fresh sweet clover leaves and flowers [10] or synthesized [11 - 13]. Sweet clover grown in sunny, arid locations typically contains higher coumarin levels than those cultivated in moist soil. Additionally, we are exploring the use of dye extracted from the green leaves of *Tectona grandis* (teak) [14, 15].

2. Material and methods

We employed the latest version of Scaps-1D, version 3.3.10 updated in 2021 [16], configured on an Intel(R) Celeron(R) N4020 CPU @ 1.10GHz - 64-bit platform for our simulations. Scaps-1D serves as a powerful tool for solving one-dimensional semiconductor equations. Developed at Ghent University (UGent), Department of Electronics and Information Systems (ELIS - Belgium), this software package is provided free of charge to the photovoltaic research community, including universities and research institutes. It was first made available to academic researchers in the photovoltaic field following the Second World Photovoltaic Conference in Vienna in 1998 [17]. Originally designed for simulating thin-film solar cells [18], Scaps-1D has evolved significantly over time. Subsequent updates incorporated features such as intra-band tunneling for heterojunction solar cells, enabling accurate simulation of transport properties across heterointerfaces [19], as well as the modeling of metastable and multivalent defects in acceptor or donor configurations [20]. Virtually all solar cell parameters can be simulated using Scaps-1D, including parameters like thickness, bandgap energy (Eg), electron affinity (χ), acceptor density (N_a), relative dielectric permittivity (ε_r), donor density (N_d), defect densities (N_t), electron mobility (μ_e), hole mobility (μ_p), conduction band densities (N_c), and valence band densities (N_v) [21]. Scaps-1D solves Poisson's equations and continuity equations for both holes and electrons [21].

2-1. Material input parameters

Table 1 : *Initial input parameter values of the semiconductors considered in the DSSC*

Parameters	FTO [1]	TiO_2 [22] :	Perovskite	Dye	Spiro-OMeTAD (variable)
Thickness (μm)	0.08	0.100	0.500	0.150	0.400
Band gap (eV)	3.50	3.2	1.90	2.50	3.06
Electron affinity (eV)	4.00	4.26	4.50	3.90	2.4
Dielectric permeability	9.00	9.00	10.00	9.00	9.00
Effective density of CB states (cm^{-3})	2.2×10^{19}	10^{19}	2.2×10^{18}	2.2×10^{18}	2.5×10^{18}
Effective density of v_b states (cm^{-3})	1.8×10^{18}	10^{19}	1.8×10^{19}	1.8×10^{19}	1.8×10^{19}
Thermal velocity of electrons (cm. s^{-1})	10^7	10^7	10^7	10^7	10^7
Hole thermal velocity ($cm.s^{-1}$)	10^7	10^7	10^7	10^7	10^7
Electron mobility ($cm^2.v^{-1}.s^{-1}$)	20	20	100	100	50
Hole mobility ($cm^2.v^{-1}.s^{-1}$)	10	10	35	35	150
Donor concentration (cm^{-3})	1×10^{19}	9.00×10^{19}	1×10^{19}	1.1×10^{15}	--
Acceptor concentration (cm^{-3})	--	--	--	1.1×10^{15}	2×10^{19}
Defect density (cm^{-3})	10^{15}	10^{15}	10^{18}	5×10^{13}	2×10^{14}

The density of interface defects between Spiro-OMeTAD/$C_{19}H_{12}O_6$, $C_{19}H_{12}O_6$/$NdRuO_3$, and $NdRuO_3$/TiO_2 is set at 10^{10} cm^{-3}. Variation in the total defect density of different materials was carried out to achieve optimum efficiency. Extensive simulation studies on perovskite cells have highlighted the critical importance of junction interface quality in determining the overall performance of solar cell architectures [23, 24]. These studies have demonstrated that high defect densities not only accelerate charge recombination rates but also degrade the quality of photovoltaic layers. In this work, the optimization of DSSC cells takes into account interface defects. Adjusting the back-contact properties with different work functions (Au = 5.1 eV, Ag = 4.7 eV, Al = 4.3 eV, Cu = 4.65 eV, Cr = 4.5 eV, Pt = 4.65 eV, Cu-graphite = 5 eV) is feasible [25, 26]. However, in our study, we maintained the back contact with an electron extraction work function of 5.1 eV for gold, as it yielded better

results with the TiO_2-based dye extracted from Hibiscus sabdariffa flowers compared to other authors [27]. The forward contact was set at 4.4 eV for TCO. The electron surface recombination velocity and hole surface recombination velocity for the back contact are 10^5 cm/s and 10^7 cm/s, respectively. For the front contact, the values are 10^7 cm/s for the electron surface recombination velocity and 10^5 cm/s for the hole surface recombination velocity.

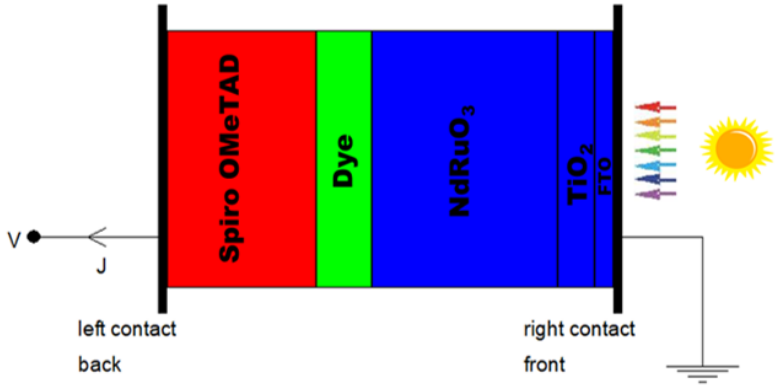

Figure 1 : *Schematic representation of the simulated p-i-n planar structure with p (red: Spiro-OMeTAD) -i (green : Coumarin) -n (bleu : $NdRuO_3/TiO_2$)*

2-2. Interface default input parameters

Table 2 : *Interface default input introduced values*

Default types	Neutral
Electron capture effective cross-section $(cm)^2$	1.00×10^{-19}
Hole cross-section capture $(cm)^2$	1.00×10^{-19}
Energy distribution	only
Reference for default energy level et	above highest eV
Energy relative to reference (eV)	0.600
Total density (integrated over all energies) $(1/cm)^2$	1.00×10^{10}

3. Results and discussion

Through the optimization of the DSSC structure, we attained an efficiency of 19.54 % with the arrangement $FTO/TiO_2/NdRuO_3$/colorant/Spiro-OMeTAD/Au, utilizing a maximum thickness of 0.5 µm for the perovskite $NdRuO_3$ structure as the photoanode. ***Figure 2***illustrates the current-voltage curve (J-V) of the DSSC cells with their initial parameter values.

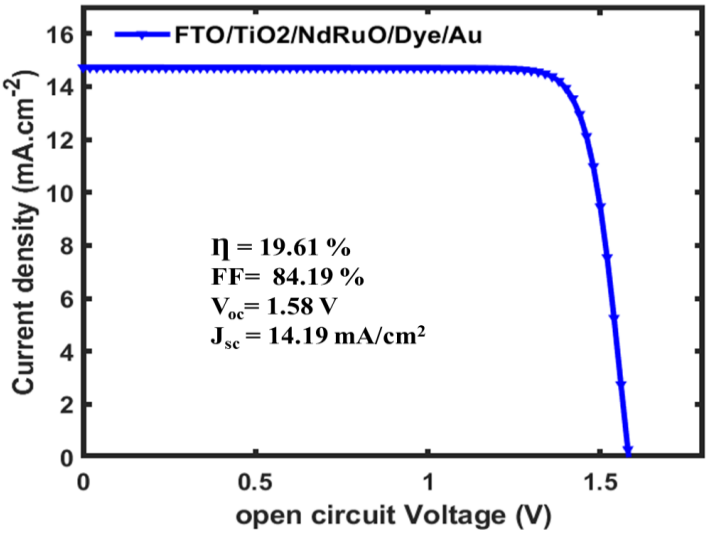

Figure 2 : *J-V curve for $NdRuO_3$ DSSC with natural dye solar cell*

Table 3 shows the results obtained using TiO_2-based photoanodes compared to the new $NdRuO_3$ based photoanode material. An increase in efficiency is observed for the $NdRuO_3$ dye-sensitized solar cell.

Table 3 : *Other results*

DSSC devices	V_{oc} (v)	J_{sc} (mA/cm²)	FF (%)	η_s (%)	reference
FTO/TiO_2 /N719/CuSCN/Ni	1.278	2.658	75.32	2.56	[28]
FTO/TiO_2/N719/Au	0.990	18.500	62.711	11.54	[29]
FTO/ZnOS/N719/Au	0.970	16.500	63.58	10.22	[29]
FTO/TiO_2/N719/Spiro-OmeTAD/Au	0.992	22.872	53.74	12.20	[7]
FTO/TiO_2/$NdRuO_3$/bis-Coumarin/Spiro-OMeTAD/Au	1.372	14.246	84.04	19.54	This work

3-1. Influence of $NdRuO_3$ gap energy

Increasing the bandgap energy of the perovskite $NdRuO_3$ structure from 1 eV to 2 eV resulted in a corresponding increase in cell efficiency from 13.07 % to 19.67 %, respectively. However, between 2 eV and 3 eV, there was no discernible change in photovoltaic parameters, followed by a subsequent drop in efficiency up to a limit of 3.75 eV, beyond which no further results were attainable. Consequently, the optimal bandgap energy is estimated to lie between 1.8 and 1.92 eV, yielding an efficiency of 19.61 % alongside a fill factor of 84.19 %, a short-circuit current (J_{sc}) of 14.2399 mA/cm², and an open-circuit voltage (V_{oc}) of 137.73 mV. The $NdRuO_3$ perovskite structure emerges as a promising candidate for use as a photoanode, owing to its bandgap properties well-suited for photovoltaic applications.

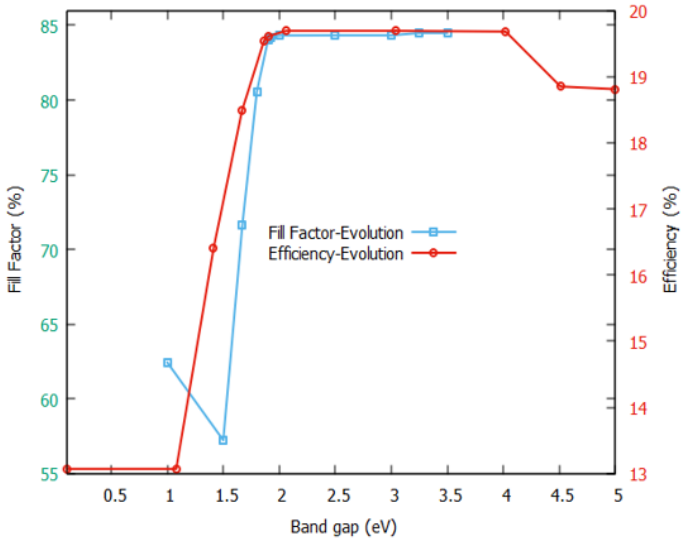

Figure 3 : *Evolution of the fill factor (FF) and cell efficiency as a function of the gap energy of the $NdRuO_3$*

3-2. Influence of perovskite $NdRuO_3$ structure thickness

Increasing the thickness of the photoanode leads to a gradual decrease in the fill factor (FF) and a simultaneous increase in the parameters V_{oc}, η, and J_{sc}, as depicted in Table 4 for these various variations. Optimal values are achieved for thicknesses ranging between 200 nm and 500 nm. The decline in fill factor (FF) and open-circuit voltage (V_{oc}) can primarily be attributed to internal recombination within the material, arising from the short lifetimes of electron and hole carriers. Similar observations have been noted in perovskite cells [30], ZnO-based DSSCs [31], and TiO_2-based DSSCs [32].

Table 4 : *$NdRuO_3$ photoanode thickness variation*

Thickness (µm)	Max V_{oc} (v)	Max J_{sc} (mA/cm^2)	FF (%)	η (%)
0.2	1.3724	14.0586	84.16	19.29
0.5	1.3716	14.2459	84.04	19.54
0.8	1.3709	14.4310	83.93	19.78
1.1	1.3702	14.6141	83.83	20.02
1.4	1.3694	14.7923	83.70	20.26
1.7	1.3685	14.9746	83.61	20.49
2	1.3676	15.1549	83.53	20.73

Table 5 : *Other reported results*

DSSC devices	V_{oc} (v)	J_{sc} (mA/cm²)	FF (%)	η_b (%)	reference
FTO/TiO_2 /N719/CuSCN/Ni	1.278	2.658	75.32	2.56	[28]
FTO/TiO_2/N719/Au	0.990	18.500	62.711	11.54	[29]
FTO/ZnOS/N719/Au	0.970	16.500	63.58	10.22	[29]
FTO/TiO_2/N719/Spiro-OmeTAD/Au	0.992	22.872	53.74	12.20	[7]
FTO/TiO_2($TiCl_4$)/$NdRuO_3$/bis-Coumarin/Spiro-OMeTAD/Au	1.372	14.246	84.04	19.54	This work

Figure 4 illustrates the current-voltage (J-V) curve for various thicknesses of the $NdRuO_3$ photoanode within the photovoltaic device. Notably, there is an efficiency enhancement by a factor of approximately 1.07, culminating in a record efficiency of 20.73 % for a natural dye solar cell. This improvement can be attributed to the incorporation of a shielding layer (acting as passivation between the substrate and perovskite structure) and the utilization of the $NdRuO_3$ inorganic perovskite structure in the natural-dye DSSC.

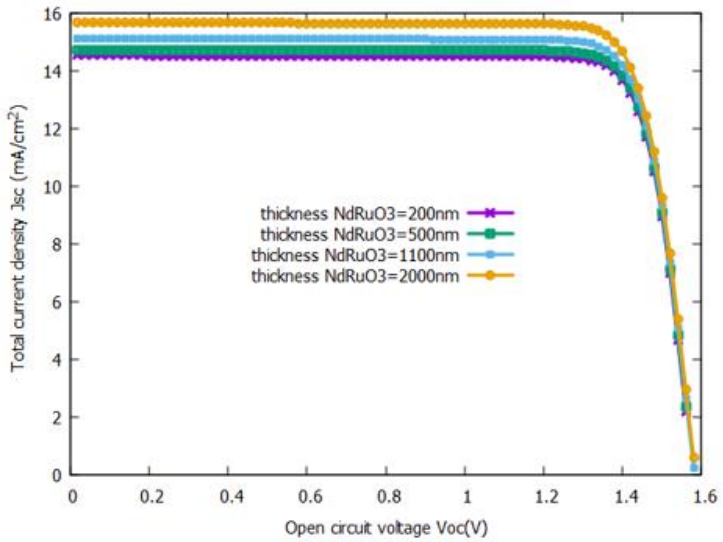

Figure 4 : *J-V curve for 4 DSSC at different $NdRuO_3$*

3-3. Influence of temperature on the solar cell

The instability of natural dye-based DSSC cells stands as a significant impediment to their widespread industrial production. It was identified both physical instability (arising from factors like temperature, UV illumination, and humidity) and chemical instability (including the degradation of dye sensitizer, electrolyte, and counter electrode, influenced by temperature, radiation, water, and oxygen) [33]. They presented various mechanisms for enhancing cell stability. A key challenge facing researchers in the photovoltaic field is the development of cells capable of operating effectively under a wide range of temperatures, both low and high, to ensure stability across diverse climatic conditions and geographical locations. In this study, we explore this temperature variation to ascertain the temperature range that optimizes the performance of natural dye DSSCs. Our findings indicate that our cells exhibit promising efficiencies at lower temperatures, as evidenced by non-negligible parameter values of V_{oc}, J_{sc}, and η at 283 K, which increase in a similar manner to those observed at ambient operating temperatures. However, we observed a decline in device quality at higher

temperatures. It is observed that the maximum conversion efficiency remains relatively constant within the range of 30-40°C, with a subsequent increase in temperature resulting in degradation of cell performance. At 70°C, there is a notable increase in recombination kinetics, leading to a reduction in cell performance [34].

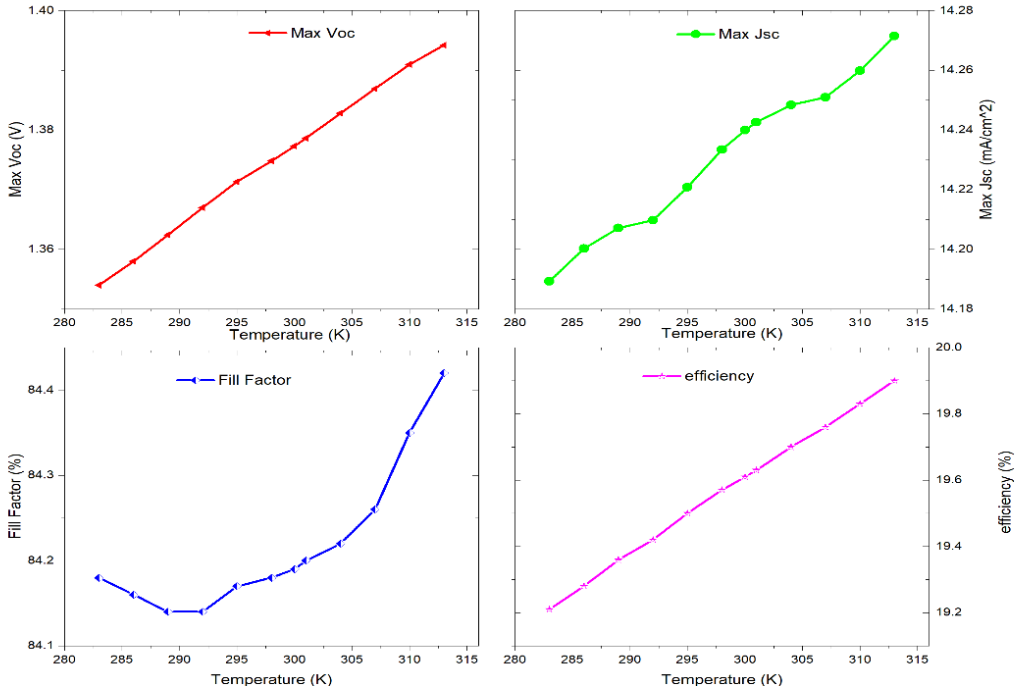

Figure 5 : *Temperature variation curve as a function of photovoltaic characteristics*

4. Conclusion

The first simulation with the Scaps-1D software of a natural dye solar cell (DSSC) in which the dye layer is responsible for light collection, through the donor-acceptor architecture via the π-bridge (D-π-A). We estimate an efficiency of 20.73 % using the extreme values of the input parameters, with a short-circuit current of 15.154 mA/cm², and an estimated open-circuit voltage of 136.79 mV. The modification of hole transport material by utilizing CuO_2 and other materials for the back contact may also be the subject of future research. Currently, we can say that it would be possible to have interesting properties for a natural dye solar cell by combining TiO_2 and $NdRuO_3$ with a hole transport material (Spiro-OMeTAD). This work offers promising prospects for synthesis. In the initial simulation using the Scaps-1D software, we investigated a natural dye solar cell (DSSC) employing a donor-acceptor architecture via the π-bridge (D-π-A) for light collection. We estimated an impressive efficiency of 20.73 % by utilizing extreme values of the input parameters, accompanied by a short-circuit current of 15.15 mA/cm² and an estimated open-circuit voltage of 136.79 mV. Future research endeavors may focus on modifying the hole transport material, potentially incorporating CuO_2 and other materials for the back contact. Currently, it appears feasible to achieve promising properties for a natural dye solar cell by combining TiO_2 and $NdRuO_3$ with a hole transport material such as Spiro-OMeTAD. This work presents exciting prospects for synthesis and further advancement in the field.

References

[1] - Y. AIT-WAHMANE, H. MOUHIB, B. YDIR, A. AIT HSSi, L. Atourki, A. IHLAL et K. BOUABID, Comparison study between ZnO and TiO2 in CuO based solar cell using SCAPS-1D, *Mater. Today Proc.*, 52 (2022) 166 - 171

[2] - N. S. NOORASID, F. ARITH, A. N. M. MUSTAFA, S. H. M. SUHAIMY, A. S. MOHD SHAH et M. A. AZAM MOHD ABID, *Numerical Analysis of Ultrathin TiO_2 Photoanode Layer of Dye Sensitized Solar Cell by Using SCAPS-1D*, IEEE Reg. Symp. Micro Nanoelectron (RSM), (2021) 96 - 99

[3] - M. Z. TOE, S.-Y. PUNG, K. A. B. YAACOB, S. S. HAN, Effect of Dip-Coating Cycles on the Structural and Performance of ZnO Thin Film-based DSSC, *Arab. J. Sci. Eng.*, 46 (2021) 6741 - 6751

[4] - A. ZATIROSTAMI, SnO_2 based DSSC with SnSe counter electrode prepared by sputtering and selenization of Sn : Effect of selenization temperature, *Mater. Sci. Semicond. Process.*, 135 (2021) 106044

[5] - B. K. KORIR, J. K. KIBET et S. M. NGARI, Simulated performance of a novel solid-state dye-sensitized solar cell based on phenyl-C61-butyric acid methyl ester (PC61BM) electron transport layer, *Opt. Quantum Electron.*, 53 (2021) 368

[6] - A. ALIZADEH, M. ROUDGAR-AMOLI, S.-M. BONYAD-SHEKALGOURABI, Z. SHARIATINIA, M. MAHMOUDI et F. SAADAT, *Dye sensitized solar cells go beyond using perovskite and spinel inorganic materials : A review, Renew. Sustain. Energy Rev.*, 157 (2022) 112047

[7] - F. JAHANTIGH et M. J. SAFIKHANI, The effect of HTM on the performance of solid-state dye-sanitized solar cells (SDSSCs) : a SCAPS-1D simulation study, *Appl. Phys. A*, 125 (2019) 276

[8] - P. GNIDA, A. SLODEK, P. CHULKIN, M. VASYLIEVA, A. K. PAJĄK, A. SEWERYN, M. GODLEWSKI, B. S. WITKOWSKI, G. SZAFRANIEC-GOROL et E. SCHAB-BALCERZAK, Impact of blocking layer on DSSC performance based on new dye -indolo[3,2,1-jk]carbazole derivative and N719, *Dyes Pigments*, 200 (2022) 110166

[9] - D. SHAHZAD, A. SAEED, M. FAISAL, F. A. LARIK, S. BILQUEES, P. A. CHANNAR, Recent Synthetic Approaches to 3,3′-(Methylene)bis(Coumarins), *Org. Prep. Proced. Int.*, 51 (2019) 199 - 239

[10] - M. A. SISAY, W. MAMMO et E. E. YAYA, PHYTOCHEMICAL STUDIES OF MELILOTUS OFFICINALIS, *BULL. Chem. Soc. Ethiop.*, 35 (2021) 141 - 150

[11] - M. M. MAKHLOUF et H. M. ZEYADA, Synthesis, structural analysis, spectrophotometric measurements and semiconducting properties of 3-phenyl azo-4-hydroxycoumarin thin films, *Synth. Met.*, 211 (2016) 1 - 13

[12] - B. MITRA, P. GHOSH, Humic acid: A Biodegradable Organocatalyst for Solvent-free Synthesis of Bis(indolyl)methanes, Bis(pyrazolyl)methanes, Bis-coumarins and Bis-lawsones, *ChemistrySelect*, 6 (2021) 68 - 81

[13] - A. D. GUPTA, S. SAMANTA, R. MONDAL et A. K. MALLIK, A Convenient, Eco-friendly, and Efficient Method for Synthesis of 3,3'-Arylmethylene-bis-4-hydroxycoumarins *"On-water,"* *Bull Korean Chem.*, (2012)

[14] - N. TIBKAWIN, N. SUPHROM, N. NUENGCHAMNONG, N. KHORANA et P. CHAROENSIT, Utilisation of Tectona grandis (teak) leaf extracts as natural hair dyes, *Color. Technol.*, (2021) cote.12594

[15] - L. RAHMAN, J. GOSWAMI et D. CHOUDHURY, Assessment of physical and thermal behaviour of chitosan-based biocomposites reinforced with leaf and stem extract of Tectona grandis, *Polym. Polym. Compos.*, 30 (2022)

[16] - C. K. BORAH, L. N. BORAH, S. HAZARIKA et A. PHUKAN, Modelling and Optimization of "n–i–p" Structured CdS/MASnI3/CdTe Solar Cell with SCAPS-1D for Higher Efficiency, *J. Electron. Mater.*, 53 (2024) 1942 - 1955

[17] - M. BURGELMAN, P. NOLLET et S. DEGRAVE, Modelling polycrystalline semiconductor solar cells, Thin Solid Films, 361 - 362 (2000) 527 - 532

[18] - M. BURGELMAN, K. DECOCK, S. KHELIFI et A. ABASS, *Advanced electrical simulation of thin film solar cells*, Thin Solid Films, 535 (2013) 296 - 301

[19] - J. VERSCHRAEGEN et M. BURGELMAN, *Numerical modeling of intra-band tunneling for heterojunction solar cells in scaps,* Thin Solid Films, 515 (2007) 6276 - 6279

[20] - M. BURGELMAN, K. DECOCK, S. KHELIFI et A. ABASS, *Advanced electrical simulation of thin film solar cells,* Thin Solid Films, 535 (2013) 296 - 301

[21] - O. ADUROJA, M. JANI, W. GHANN, S. AHMED, J. UDDIN et F. ABEBE, Synthesis, Characterization, and Studies on Photophysical Properties of Rhodamine Derivatives and Metal Complexes in Dye-Sensitized Solar Cells, *ACS* Omega, 7 (2022) 14611 - 14621

[22] - H. TANG, K. PRASAD, R. SANJINÈS, P. E. SCHMID et F. LÉVY, Electrical and optical properties of TiO_2 anatase thin films, *J. Appl. Phys.*, 75 (1994) 2042 - 2047

[23] - N. DEVI, K. A. PARREY, A. AZIZ et S. DATTA, Numerical simulations of perovskite thin-film solar cells using a CdS hole blocking layer, *J. Vac. Sci. Technol. B*, 36 (2018) 04G105

[24] - Y. GAN, X. BI, Y. LIU, B. QIN, Q. LI, Q. JIANG et P. MO, Numerical Investigation Energy Conversion Performance of Tin-Based Perovskite Solar Cells Using Cell Capacitance Simulator, *Energies*, 13 (2020) 5907

[25] - A. HUSAINAT, W. ALI, P. COFIE, J. ATTIA, J. FULLER, A. DARWISH, Simulation and Analysis Method of Different Back Metals*, J. Opt. Photonics,* 8 (2020)

[26] - N. D. LAM, Modelling and numerical analysis of ZnO/CuO/Cu_2O heterojunction solar cell using SCAPS, *Eng. Res. Express*, 2 (2020) 025033

[27] - S. C. YADAV, A. SHARMA, R. S. DEVAN et P. M. SHIRAGE, Role of different counter electrodes on performance of TiO_2 based dye-sensitized solar cell (DSSC) fabricated with dye extracted from Hibiscus Sabdariffa as sensitizer, *Opt. Mater.*, 124 (2022) 112066

[28] - O. V. ALIYASELVAM, S. M. JUNOS, F. ARITH, N. IZLAN, M. M. SAID et A. N. MUSTAFA, *Optimization of Copper (I) Thiocyanate as Hole Transport Material for Solar Cell by Scaps-1D Numerical Analysis »*, *Przegl*, (2022) 133 - 137

[29] - B. K. KORIR, J. K. KIBET et S. M. NGARI, Computational Simulation of a Highly Efficient Hole Transport-Free Dye-Sensitized Solar Cell Based on Titanium Oxide (TiO2) and Zinc Oxysulfide (ZnOS) Electron Transport Layers, *J. Electron. Mater.*, 50 (2021) 7259 - 7274

[30] - Q. CHEN, Y. NI, X. DOU, Y. YOSHINORI, The Effect of Energy Level of Transport Layer on the Performance of Ambient Air Prepared Perovskite Solar Cell : A SCAPS-1D Simulation Study, *Crystals*, 12 (2022) 68

[31] - E. KOUHESTANIAN, M. RANJBAR, S. A. MOZAFFARI et H. SALARAMOLI, Investigating the effects of thickness on the performance of ZnO-based DSSC, *Prog. Color Color. Coat.*, 14 (2021) 101 - 112

[32] - M. M. ABDEL-GALEIL, R. KUMAR, A. MATSUDA et R. E. EL-SHATER, Investigation on influence of thickness variation effect of TiO_2 film, spacer and counter electrode for improved dye-sensitized solar cells performance, *Optik,* 227 (2021) 166108

[33] - F. KABIR, S. MANIR, MD. M. H. BHUIYAN, S. AFTAB, H. GHANBARI, A. HASANI, M. FAWZY, G. L. T. DE SILVA, M. R. MOHAMMADZADEH, R. AHMADI, A. ABNAVI, A. M. ASKAR et M. M. ADACHI, Instability of dye-sensitized solar cells using natural dyes and approaches to improving stability – An overview, *Sustain. Energy Technol. Assess.*, 52 (2022) 102196

[34] - S. R. RAGA, F. FABREGAT-SANTIAGO, *Temperature effects in dye-sensitized solar cells, Phys. Chem.,* 15 (2013) 2328

[35] - T. SUTRADHAR et A. MISRA, The role of π-linkers and electron acceptors in tuning the nonlinear optical properties of BODIPY-based zwitterionic molecules, RSC Adv., 10 (2020) 40300 - 40309